Draft version May 9, 2016
Preprint typeset using LaTeX style emulateapj v. 01/23/15

GRAVITATIONAL WAKE OF M33 IN THE DARK MATTER HALO

W. Yingling[1]
Steward Observatory, University of Arizona, Tucson, AZ 85719

G. Besla[1]
Steward Observatory, University of Arizona, Tucson, AZ 85719

Draft version May 9, 2016

ABSTRACT

In this project we investigated the effects of the dark matter halo of M31 and the Milky Way on the satellite galaxy, M33.

Keywords: galaxies: halo, dark matter, satellites, simulation galaxies: individual(M33, Milky Way, M31)

1. INTRODUCTION

A continuing problem in today's galactic field is the investigation of gravitational wake experienced by small dynamical bodies. The wake is product of two dynamical bodies interacting and passing through each other. The forces of dynamical friction (DF) act to slow the trajectory of two bodies. In the context of one large body and a comparatively small one, the smaller one feels a significantly larger drag force and instead of orbiting the larger body, it tends to spiral inwards. In this paper I attempt to show the wake

It is of particular interest to be able to model the wake of small dynamical bodies through significantly larger bodies so that we can have a better understanding of how they interact. With this knowledge, we can better predict the morphology of our own galaxy and also understand how other galaxies got their current shape with an emphasis on how satellites particularly can shape the halo, disk, and bulge.

We inquire about this topic to hope to gain a clearer picture of how satellite galaxy M33 is going to inspiral and eventually merge with the merged product of the Milky Way (MW) and M31. It is currently unclear if there are resonances created as result of satellites passing the the dark matter (DM) halo. Finding out more about the wake could help elucidate that.

In previous literature, Mulder in 1983 attempts to show the effects of DF by modeling an ideal case where a point mass moves through a Maxwellian Distribution sea of particles. The point mass is less in size than the entire surrounding sea of particles. In Figure 1, we see that there is a general over density in the plot directly behind the point mass. It can also be noted that the over density begins appearing in front of the mass and then expanding outward. However this simulation is only modeling the system in 2-dimension and so therefore is not account for a third dimension. This does point in the right direction and allows us to see where we should look for the wake where it will be densest. Figure 1 is what we will be trying to replicate with the modification of being in 3 dimensions.

Additionally, Weinberg conducted a handful of studies where he investigated DF and how it related to the wake and sought to answer how resonances in the halo might effect the disk. The conclusion was that as a satellite passes through the halo, it localizes particles to the path taken by the satellite and the over density in turn can create distortions in the disk of a spiral galaxy (Weinberg 1998). Weinberg also shows that warping can happen in disks and also notes that the warp happens after some lag time because the disk needs time to respond to the changing halo and the generally large distances at which gravity is felt from (Weinberg 1998). This warping is characteristically at opposite edges of the disk according to (Weinberg 1998).The causes of warping can occur for a number of reasons. The main four reasons of warping are from excitation in the halo, gravitational noise in the halo, the Coriolis force the disk, and tidal fields from satellites according to (Nelson & Tremaine 1995). We will only be concerned with the excitation in the halo for this paper.

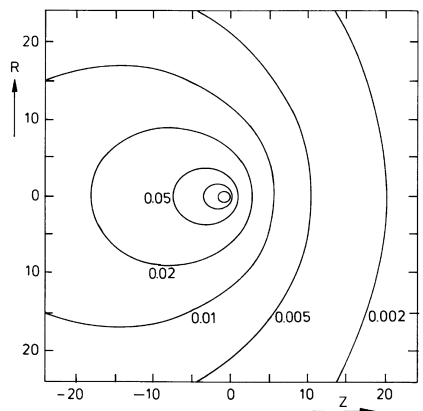

Figure 1. Over Density plot point mass traveling through sea of particles in 2-dimensions. The numbers located on the contours refers to the ratio of local over density subtracted by the average density of the sea. From (Mulder 1983).

2. THIS PROJECT

For this project, we sought out to determine if the gravitational wake could be seen at all from our analysis. We wanted to answer if the wake was noticeable at the resolution of one million particles and if we could deter-

yinglingw@email.arizona.edu

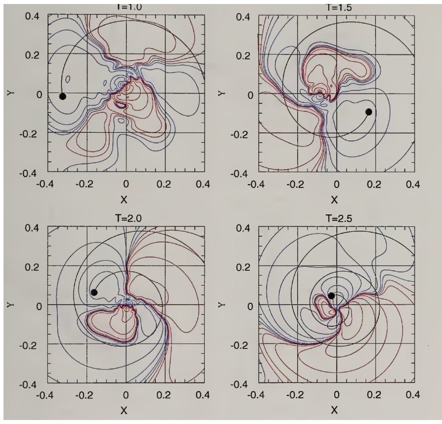

Figure 2. Over Density plot from Choi shoing inner and outer wake in 2-dimensions. Red contours refer to an over density and blue refers to and under denstity. The black line represents the trajectory of the point mass inspiraling.From top left to bottom right the time is progressing forwards. From (Choi 2007).

mine any tendencies for resonances within halo based off of the path taken from M33.

The question of whether the wake is visible is a question and check for the simulation that we are using given by (van der Marel, Besla 2012). In the best case scenario, we would be able to emulate the simulation provided in the thesis of (Choi 2007). In this thesis, and shown in Figure 2, we can identify an inner and outer wake. However, it was hopeful that we would be able to see its effects in the simulation.

The question we hope to answer with this project is how apparent the wake will be through the simulation presented by (van der Marel, Besla 2012). This is critical for analysis because it will lead us to have a better understanding of what is happening to M33 as it orbits in the dark matter halo.

3. METHODS

For this project, we used the simulation presented by (van der Marel, Besla 2012). In the highest resolution form of the simulation by (van der Marel, Besla 2012) is on order of one million particles. This simulation is thought to be to most accurate simulation of the merger sequence between M31 and the MW to date. However, it may have too few in particles in order to exhibit the characteristics of the wake for M33. The simulation fully includes the different components of the MW, M31, and M33. For the purposes of this project, we only consider the dark mater halo from the MW and M31.

The code I have written for this analysis was written in Python. It takes the center of mass (COM) of the M33 and M31. It then subtracts out the relative position of M31 and M33 so it appears as if M33 is at the origin our plot. in

4. HELICITY AMPLITUDES

It has been realized that helicity amplitudes provide a convenient means for Feynman diagram[1] evaluations. These amplitude-level techniques are particularly convenient for calculations involving many Feynman diagrams, where the usual trace techniques for the amplitude squared becomes unwieldy. Our calculations use

[1] Footnotes can be inserted like this.

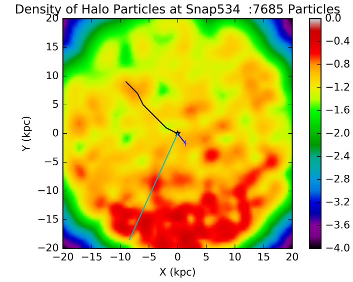

Figure 3. Plot of the combined halos, where M33 is at the center. The black star represent the COM of M33. The blue line with a plus symbol at the end is a scaled representation of the velocity. The green line is pointing to the COM of M31. The black line is showing the previous path of M33. The colors are a logarithmically scaled density of the combined halo.

the helicity techniques developed by other authors (**?**); we briefly summarize below.

4.1. *Formalism*

A tree-level amplitude in e^+e^- collisions can be expressed in terms of fermion strings of the form

$$\bar{v}(p_2,\sigma_2)P_{-\tau}\hat{a}_1\hat{a}_2\cdots\hat{a}_n u(p_1,\sigma_1), \tag{1}$$

where p and σ label the initial $e^{\pm}$ four-momenta and helicities ($\sigma=\pm1$), $\hat{a}_i = a_i^{\mu}\gamma_{\nu}$ and $P_{\tau}=\frac{1}{2}(1+\tau\gamma_5)$ is a chirality projection operator ($\tau=\pm1$). The a_i^{μ} may be formed from particle four-momenta, gauge-boson polarization vectors or fermion strings with an uncontracted Lorentz index associated with final-state fermions.

In the chiral representation the γ matrices are expressed in terms of 2×2 Pauli matrices σ and the unit matrix 1 as

$$\gamma^{\mu} = \begin{pmatrix} 0 & \sigma_+^{\mu} \\ \sigma_-^{\mu} & 0 \end{pmatrix}, \gamma^5 = \begin{pmatrix} -1 & 0 \\ 0 & 1 \end{pmatrix},$$
$$\sigma_{\pm}^{\mu} = (\mathbf{1}, \pm\sigma),$$

giving

$$\hat{a} = \begin{pmatrix} 0 & (\hat{a})_+ \\ (\hat{a})_- & 0 \end{pmatrix}, (\hat{a})_{\pm} = a_{\mu}\sigma_{\pm}^{\mu}, \tag{2}$$

The spinors are expressed in terms of two-component Weyl spinors as

$$u = \begin{pmatrix} (u)_- \\ (u)_+ \end{pmatrix}, v = ((v)_+^{\dagger}, (v)_-^{\dagger}). \tag{3}$$

The Weyl spinors are given in terms of helicity eigenstates $\chi_{\lambda}(p)$ with $\lambda=\pm1$ by

$$u(p,\lambda)_{\pm} = (E\pm\lambda|\mathbf{p}|)^{1/2}\chi_{\lambda}(p), \tag{4}$$
$$v(p,\lambda)_{\pm} = \pm\lambda(E\mp\lambda|\mathbf{p}|)^{1/2}\chi_{-\lambda}(p) \tag{5}$$

5. FLOATING MATERIAL AND SO FORTH

Consider a task that computes profile parameters for a modified Lorentzian of the form

$$I = \frac{1}{1+d_1^{P(1+d_2)}} \tag{6}$$

where

$$d_1 = \sqrt{\left(\frac{x_1}{R_{maj}}\right)^2 + \left(\frac{y_1}{R_{min}}\right)^2}$$

$$d_2 = \sqrt{\left(\frac{x_1}{PR_{maj}}\right)^2 + \left(\frac{y_1}{PR_{min}}\right)^2}$$

$$x_1 = (x - x_0)\cos\Theta + (y - y_0)\sin\Theta$$

$$y_1 = -(x - x_0)\sin\Theta + (y - y_0)\cos\Theta$$

In these expressions x_0,y_0 is the star center, and Θ is the angle with the x axis. Results of this task are shown in table 1. It is not clear how these sorts of analyses may affect determination of $M_\odot$, but the assumption is that the alternate results should be less than 90° out of phase with previous values. We have no observations of Ca II. Roughly $\frac{4}{5}$ of the electronically submitted abstracts for AAS meetings are error-free.

We are grateful to V. Barger, T. Han, and R. J. N. Phillips for doing the math in section 4.1. More information on the AASTeX macros package is available at http://www.aas.org/publications/aastex. For technical support, please write to .

Facilities: Nickel, HST(STIS), CXO(ASIS).

APPENDIX

APPENDIX MATERIAL

Consider once again a task that computes profile parameters for a modified Lorentzian of the form

$$I = \frac{1}{1 + d_1^{P(1+d_2)}} \tag{A1}$$

where

$$d_1 = \frac{3}{4}\sqrt{\left(\frac{x_1}{R_{maj}}\right)^2 + \left(\frac{y_1}{R_{min}}\right)^2}$$

$$d_2 = \frac{3}{4}\sqrt{\left(\frac{x_1}{PR_{maj}}\right)^2 + \left(\frac{y_1}{PR_{min}}\right)^2} \tag{A2}$$

$$x_1 = (x - x_0)\cos\Theta + (y - y_0)\sin\Theta \tag{A3}$$

$$y_1 = -(x - x_0)\sin\Theta + (y - y_0)\cos\Theta \tag{A4}$$

For completeness, here is one last equation.

$$e = mc^2 \tag{A5}$$

REFERENCES

Mulder, R. 1983, A&A, 117, 9-16
Weinberg, M. D. MNRAS, 299, 449-514,

Figure 4. Derived spectra for 3C138 (see **?**). Plots for all sources are available in the electronic edition of *The Astrophysical Journal*.

Nelson, R., & Tremaine, S. 1995, ApJL, 277, L49
van der Marel, Besla, G. 2012,
Choi, Jun-Hwan, 2007, PhDThesis,
Garavito, N. et al 2016, in preparation

Figure 5. A panel taken from Figure 2 of **?**. See the electronic edition of the Journal for a color version of this figure.

Figure 6. Animation still frame taken from **?**. This figure is also available as an mpeg animation in the electronic edition of the *Astrophysical Journal*.

Note. — We can also attach a long-ish paragraph of explanatory material to a table.

Table 1
Sample table taken from **?**

POS	chip	ID	X	Y	RA	DEC	IAU$\pm$ δ IAU	IAP1$\pm$ δ IAP1	IAP2 $\pm$ δ IAP2	star	E	Comment

Note. — Table 1 is published in its entirety in the electronic edition of the *Astrophysical Journal*. A portion is shown here for guidance regarding its form and content.

[1] Sample footnote for table **??** that was generated with the LaTeX table environment
[2] Yet another sample footnote for table **??**
[3] Another sample footnote for table **??**

Table 1 — *Continued*

POS	chip	ID	X	Y	RA	DEC	IAU ± δ IAU	IAP1± δ IAP1	IAP2 ± δ IAP2	sta

References. — (1) Mulder 1983; (2) Weinberg 1998; (3) Nelson & Tremaine 1995; (4) van der Marel, Belsa 2012; (5) Choi 2007; (6) Garavito 2016

[a] Sample footnote for table 1 that was generated with the deluxetable environment

[b] Another sample footnote for table 1